1 Background

Classical molecular dynamics simulations were performed to analyze the interface formed between various aqueous salt solutions and CCl_4 . Three salt solutions were simulated, as well as a reference system consisting of neat-H_2O for comparison to previous computational efforts.[1–6] The salts used in the simulations were NaCl, $NaNO_3$, and Na_2SO_4. These were chosen to compare to the recent experimental sum frequency generation (SFG) spectroscopy results for the same systems,[7] and to supplement those experiments with additional molecular-level information. Analyses were performed on the simulation data to extract ionic and molecular density data, information about water orientation near to the interface, and simulated SFG spectra. The analyses are similar to, and logical extensions of previous computational work done on aqueous salt systems.

1.1 Density Profiles

Density histograms of simulated interfaces have been used in previous publications to show ionic and molecular distribution behavior in various systems.[2,4,6,8–12] In this work the density profile of water throughout the interface is fitted to a hyperbolic tangent function[11,13] as shown here:

$$\rho(z) = \frac{1}{2}(\rho_1 + \rho_2) - \frac{1}{2}(\rho_1 - \rho_2)\tanh\left(\frac{z - z_0}{d}\right) \tag{1}$$

Equation (1) relates the interfacial density, ρ, as a function of position, z, along a given system reference axis, to the densities of the phases on either side of the location of the Gibb's dividing surface, z_0. The bulk density ρ_1 and the density within the second phase, ρ_2 are fitted. The interfacial width, d, is related to the "90-10" thickness that is often reported by $t = 2.197d$.

These measures of interfacial thickness provide a means of comparing the depths to which the water phase is affected by ions located at the interface. The density distributions of the salts depict concentration and depletion phenomena throughout the interfacial region, and also serve to illustrate ionic affinity within this region. Previous work has been performed on the air-water interface with various ions introduced, showing varying levels of interfacial affinity, with the more polar ions being the most interfacially active. We present the density distribution results below for the neat-H_2O and salt solutions interfaced with an organic CCl_4 phase.

1.2 Molecular Orientation

Several methods have been used previously to show molecular orientation profiles of water molecules throughout simulated interfacial regions.[1,2,11,14–19] In this work we have chosen to compute the orientation of water using two vectors that describe the orientation in space given the locations of the three atoms comprising the molecule. The molecular bisector, a vector that points along the axis of symmetry of the water molecule from the hydrogen-end to the oxygen, provides directional orientation of the molecule in an intuitive way. A

second vector, what is refered to here as the molecular normal vector, is established as the vector pointing normal to the plane formed by the three atoms of the water molecule and establishes its "tilt". Analyzing the angle made between these two vectors and a given space-fixed reference axis (herein defined as the long-axis of the simulation cells, oriented perpendicular to the interfacial plane and pointing out of the aqeuous phase) is a means of finding the orientation of waters within these simulated systems as illustrated in figure 1. The angle formed between the molecular bisector and the reference axis will hereafter be referred to as θ, and the molecular normal vector as ϕ. The analysis in this work reports the cosines of these two angles, and because of the symmetry of the water molecule where the hydrogens are not uniquely identified, the cosines of the two angles are limited as follows: $-1 \leq \theta \leq 1$ and $0 \leq \phi \leq 1$. We report here two-dimensional histograms showing the orientation profiles of θ and ϕ as functions of the distance from the gibbs dividing surface of the interface, as found from the fitting in our density profile analyses.

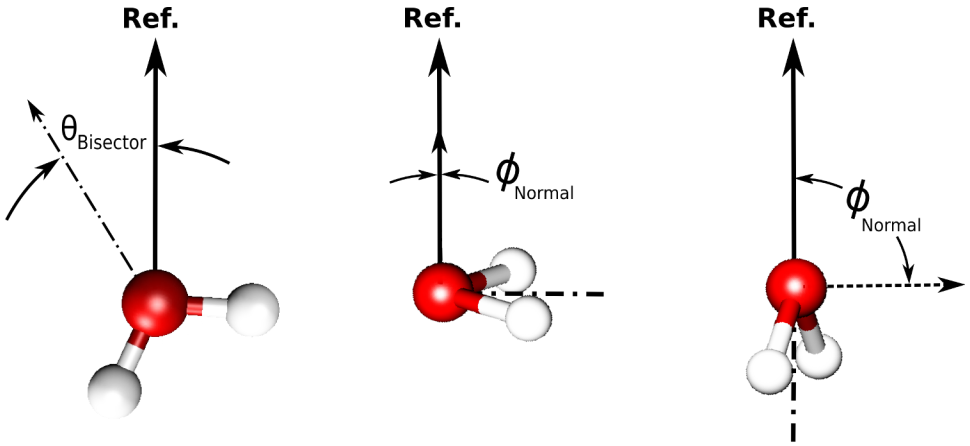

Figure. 1 — Angles used to define molecular orientation. The system reference (Ref.) axis is that which is perpendicular to the plane of the aqueous-organic interface, and points out from the aqueous phase into the organic one. The molecular bisector vector points from the hydrogen-end of the water to the oxygen end, and orients along the axis of symmetry. The angle it forms with the reference axis is either aligned or anti-aligned such that $-1 \leq \cos\theta \leq 1$. The angle formed between the vector normal to the molecular plane (formed by the three water atoms) and the reference-axis orients the "twist" of the molecule such that $0 \leq \cos\phi \leq 1$, where the water molecular plane is either laying flat on the interface ($\cos\phi = 1$) or it the water is perpendicular to the interface ($\cos\phi = 0$).

1.3 Computational SFG

A difficult challenge for experimental surface studies is in understanding the vibrational spectroscopy of liquid water. Hydrogen bonding between water molecules causes intermolecular and intramolecular couplings.

Simulations provide the analytical capacity to relate the broad lineshapes, and the often difficultly-assessed impact of hydrogen bonding as a function of OH vibrational frequency, to microscopic geometries, forces, and environments. In this work we compute the SFG spectra of the interface between the salt solutions and an orgnanic phase to qualify the conclusions of a previous experimental work by our group,[7] and to elucidate some of the microscopic phenomena that lead to water's spectroscopic signatures.

The computational method used in this work is based on that of Morita and Hynes[20] as outlined in a previous study by this group utilizing the same technique.[21] The computational SFG technique has been improved in more recent studies by Morita et al,[22,23] and with other enhanced water models. The technique used in this work has been established to recreate the qualities of the experimental spectra to a sufficient degree such that we may still draw qualified conclusions about lineshape and intensity. The most dramatic short-coming of the current technique is that of reproducing accurately the lower-frequency features of the SFG spectra below the 3200 cm^{-}1 region. However, our present analysis is concerned primarily with the overall intensity and response, and thus we still draw qualitative conclusions based on our computed results, and utilize the simpler computational methods of our previous works.

2 Computational Setup

The molecular dynamics methods used in this work are similar to those from our previous computational efforts with some modifications described below.[1,2,4] Simulations were carried out using the Amber 9 software package. The polarizable ion model parameters are taken from previous works on similar systems.[8,14,24–26] The polarizable POL3 model was used for water molecules.[27] Fully polarizable models have been used in previous interface simulation studies because they are known to more accurately reproduce interfacial structure and free energy profiles.[15,28–31]

A total of 4 systems were simulated consisting of aqueous salt and CCl_4 phases. A slab geometry was used to produce two interface regions within each simulation cell.[1] The results of the analyses performed herein on each simulated system made use of the natural symmetry of the two interfaces by averaging the results from the two surfaces. The organic region was formed in a box 30 Å on a side with 169 CCl_4 molecules to reproduce a standard temperature density of 1.59 $\frac{g}{mL}$. The aqueous region was formed in a box 30x30x60 Å^3, with the long axis perpendicular to the interfaces. The number of water molecules and ions varied for each system in order to reproduce a concentration of 1.2 M. The specific populations of each molecule are listed in table 2. The organic and aqueous boxes were then joined to form a system 90 Å long with interface areas of 30x30 Å^2.

System	H_2O	Cation	Anion
Neat Water	1800	0	0
NaCl	1759	40	40
$NaNO_3$	1732	40	40
Na_2SO_4	1740	86	43

Table 1 — Aqueous molecule and ion numbers. Listed are the populations of each component for the 4 simulated aqueous phases. All systems were simulated at near 1.2 M salt concentrations.

The water, salts, and CCl_4 were each randomly packed into their respective boxes with a minimum packing distance of 2.4 Å . After joining the aqueous and organic phases and forming the two interfaces, the total system was energy minimized using a conjugate gradient method. Following minimization, the system was equilibrated at a constant temperature of 298 K with weak coupling to a heat bath for a period of 10 ns, using a simulation timestep of 1.0 fs. A non-bonded potential cutoff of 9.0 Å was used. Following equilibration the system was simulated with the same parameters for a further 10 ns with atomic position data recorded every 50 fs. This resulted in a total of 200,000 snapshots which were used in the data analysis.

3 Component Densities

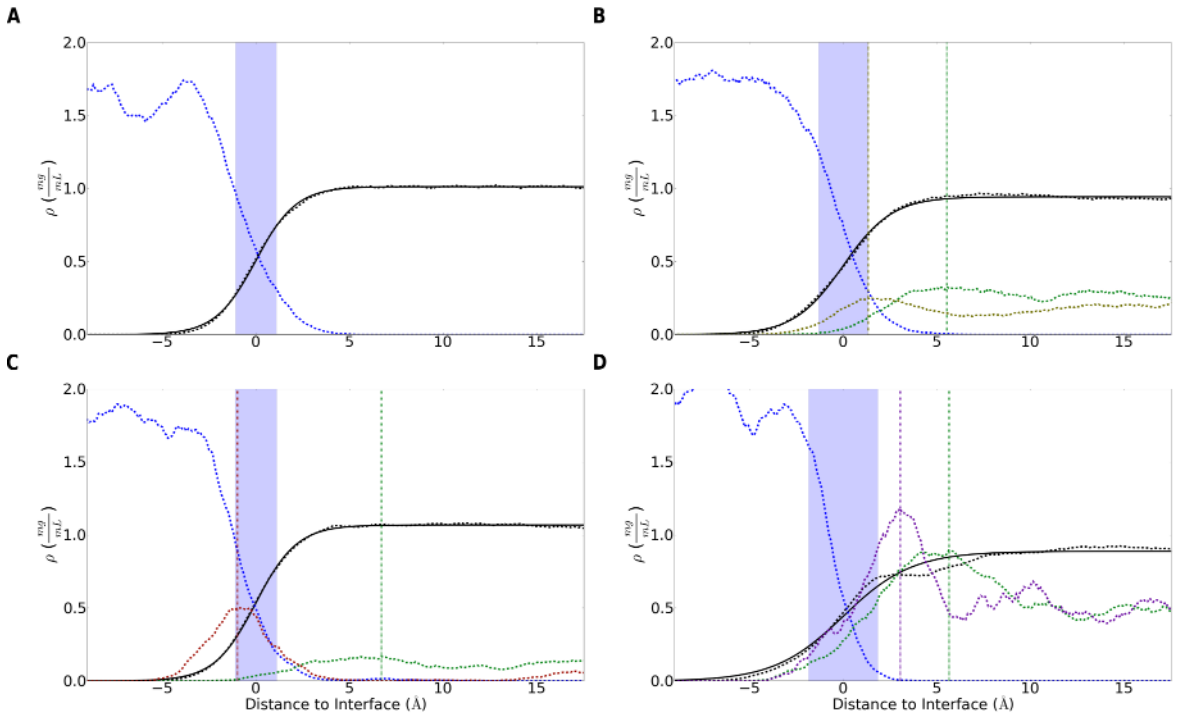

Figure. 2 — Aqueous salt and CCl_4 density profiles. The gibbs dividing surface location, z_0, were designated as the 0.0 Å location, and all lineshapes are plotted as distances to the gibbs interface. Neat-H_2O (A), NaCl (B), $NaNO_3$ (C), and Na_2SO_4 (D) salt-system densities are plotted with the water-oxygen density (dashed black) and the corresponding fitted lineshape (solid black). Each interfacial width, d, is designated as a highlighted blue region of width d centered about z_0. The CCl_4 (dashed blue), Na^+ cation (dashed green) and respective anion densities are also shown for each system. The scaling of the cation (10x) and anion (5x) densities was used to clarify their peak and trough locations. The maxima of the ionic components are marked with dashed vertical lines of the same colors to show relative component locations within the interfacial region.

The component density profiles of each system were calculated to study the effects of adding salts and to find deviations from the neat-H_2O /CCl_4 system. The water density profile of each system was fitted to a hyperbolic tangent (Eq. 1), and the all the density profiles were plotted as distances from each of the gibbs dividing surface locations, z_0. The resulting plots are shown in figure 2. z_0 of each system was shifted to a location of 0.0 Å , and the interfacial thickness, d, is visualized by a blue shaded region of the respective thickness centered about z_0. The widths of the interfacial regions for the neat-H_2O (A), NaCl (B), $NaNO_3$ (C), and Na_2SO_4 (D) systems are 2.16, 2.62, 2.20, and 3.69 Å respectively. In each of the salt solutions, the peak in the anionic density profile occurs closer to the CCl_4 phase than the corresponding cationic peak.

Various parameters of interest such as the interfacial thicknesses, ionic component locations, and relative distances between the peaks of the ion profiles are collected in table 2.

System	d	Anion	Cation	Anion-Cation Distance
Neat-H_2O	2.16	-	-	-
NaCl	2.62	1.33	5.53	4.20
$NaNO_3$	2.20	-0.99	6.71	7.70
Na_2SO_4	3.69	3.04	5.64	2.60

Table 2 — Aqueous salt system density parameters. Interfacial widths, d, and the locations of the maxima of the density profiles for each ionic component are listed for the simulated salt systems. The relative distances between the anion and cation density peak locations are listed to show how the different anions affect the relative location of their cationic counterions.

The oscillations in the surface density profiles of water and the adjoining organic liquid phase have been noted previously and attributed to thermal capillary waves on a larger length-scale than the simulated system size.[32] The same work also made note that the interfacial thickness is size-dependent on the interfacial surface area. Increasing the surface area dimensions should cause an increase in the interfacial width. Two works on the H_2O -CCl_4 surface offer direct comparison of this.[2,32] In comparing the interfacial widths, there is an increase in width as the system cross-sectional area is increased. This phenomenon implies that care must be taken when making quantitative comparisons between simulation studies.

The neat-H_2O system is the acting benchmark and has been simulated previously.[2,11,17] Deviations in width of the interface from the pure-water system can be attributed to the added ions in the solution. In comparing the three salt solutions, any differences in those systems are anionic in nature because the cation of each system was kept the same. NaCl is the simplest of the three salts with a monatomic and monovalent anion. The peak of the anion density profile is within the aqueous phase and is found on the aqueous-side of the interfacial width. The location of the cation density peak is, as mentioned above, deeper into the aqueous phase than the anion by over 4 Å . This layering of ions within the aqueous phase is attributed to the break in the anisotropy of the field of the bulk region upon introduction of the second (organic) phase. The more polarizable and negatively charged anions move towards the interface to effectively screen the charge of the organic phase and the more highly ordered water structure near to it. The counterions then are drawn towards the negative charge built up by the anions to create the second ion density peak deeper into the aqeuous phase. The overall shape of the water profile in the NaCl system is relatively unaffected (relative to the neat-H_2O) as the bulk water density is unchanged, and the width of the interface is increased by 18% from that of system A.

The $NaNO_3$ system introduces the monovalent, polyatomic nitrate anion. The location preference of nitrate is a contentious subject that has been studied much in recent years. Experimental works have been performed using a few surface-sensitive techniques. One work used SFG to detect structural changes in the water hydrogen-bonding network in the presence of the anion, and found that it affects the SFG signal

intensity from the interface, but could not create the anion density profile[33]. The same work found SFG intensity enhancement for hydrogen-bonded water following a trend of $H_2SO_4 \geq HCl > HNO_3$. Strengthening of the interfacial hydrogen-bonding structure of water would allow it to further penetrate into a second, organic phase, thus widening the interface region, and enhancing the SFG intensity from the interface from hydrogen-bonded species. We find the same trend when comparing interfacial widths from our simulations. In the case of the nitrate anion location, however, the SFG studies stopped short of reporting a concentration profile. A recent X-ray photoemission spectroscopy study was performed to specifically determine the nitrate concentration profile for the water-vapor interface, and reported the current differences of opinion between recent experiment and simulation.[34] The XPS results reported a surface depletion of the nitrate anion relative to the bulk, similar to previous MD simulations of the same systems. Other works find similar nitrate surface depletions,[35] but were performed on the liquid-vapor interface, and help to contrast the effect of the presence of an organic phase as in the present work. We find a surface enhancement of the nitrate anion located further into the organic side of the interface. The nitrate density peak is located the furthest out from the aqueous phase of the three salt systems. The location of the sodium cation peak is a significant distance further into the bulk from the anion than either of the NaCl or Na_2SO_4 systems. Such surface location and enhancement of the nitrate ion suggests a very strong interaction with the interface waters, breaking the hydrogen-bonding network near to the organic phase, and also strongly screening the field of the CCl_4 molecules from the interface. This accounts for the narrower interfacial width as the water can no longer extend a bonded network into the organic phase. However, as the water is strongly interacting with the nitrate and effectively screening the surface charge from the bulk, the cation is less attracted to the interface and the ionic double-layer is widened. Xu, et al, studied this phenomena finding a lack of ion-pairing of various nitrates at the air-water interface.[36] They found that solvation from an abundance of water at the interface weakens coulombic forces between ions, leading to greater cation-anion separation. They concluded that the surface nitrate is dehydrated, and the water provides adequate shielding of the ionic coulombic interactions. It is reasonable to assume that this same effect may cause the greater cation-anion separation at the interface of the $NaNO_3$ system, even in the presence of the organic phase.

For monovalent ions at the CCl_4 -H_2O interface, the behavior is completely different than for the air-H_2O systems. Previous works found concentrations of monovalent anions to be lower at the CCl_4 -H_2O interface than at the air-liquid one.[37] However, larger and more polarizable anions were found to be less solvated and more surface active than smaller ones such as Cl^- . I^-, for instance, has more contact with the CCl_4 phase because of a more exposed surface area and higher polarizability, resulting in repulsion of the CCl_4 , and a wider aqueous interface. The exposure to the CCl_4 phase decreases the anion concentration relative to the air-water interface, yet a very prominent density peak remains at or near the interface for those larger and polarizable ions.

The widest interface is that of the Na_2SO_4 solution, indicating that the SO_4^{2-} anions act to affect greatly the hydrogen bonding network between the surface waters. The location of the sulfate density enhancement is the furthest into the aqueous bulk of the three anions, as previously observed,[31] and the divalent and

highly polarizable nature of the anion appears to attract the counterion closest for the narrowest sub-surface ionic double-layer. This attraction is likely coulombic, and the charge screening that separates the ion pairs in the $NaNO_3$ solution is not present in aqueous Na_2SO_4 . Although the geratest concentration enhancement is further into the bulk region, seemingly outside the region designated by the width, the water network is still greatly enhanced. This has been verified by an increase in SFG response of the surface waters relative to the neat-water system in a recent work by this group [7]

Most of the recent studies on ion concentration near water interfaces have noted that large and polarizable ions will concentrate at the surface,[9,29,38,39] while small non-polarizable ion tend to be repelled. The surface enhancement calculated from molecular dynamics, however, portrays the lower bound of the actual effect because of the reduced polarizability values used in simulations to avoid the so-called "polarization catastrophe." The enhancement of surface anions is also believed to be the cause of the subsurface cation density increase. The counterions are attracted to the concentrations of anions at the surface, which are in turn stabilized by the increased polarization of the water due to the distorted interfacial electric field. The affinity for the surface follows the trend of surface tension increments, $\frac{d\gamma}{dm_2}$, where $Na_2SO_4 > NaCl > NaNO_3$.[38] This also follows the hoffmeister series trend for anions found to be the most "structure-making", and they are found to be density enhanced further into the interface.

4 Water Orientation

The orientation of water within the aqueous/organic interface of the system was defined using the angles formed by molecular axes and the fixed reference axis of the system (perpendicular to the interfacial plane). The two molecular axes used are the water bisector, pointing from the hydrogen side to the oxygen, and the vector normal to the plane formed by the three atoms of the water molecule, as depicted in figure 1. Figure 3 shows the angle profiles of both the molecular bisector and the molecular plane normal of water molecules relative to the system reference axis at various depths into the aqueous phase. Darker red regions of the plots indicate higher orientational populations, while homogeneous coloring across the angle range indicates orientational isotropy.

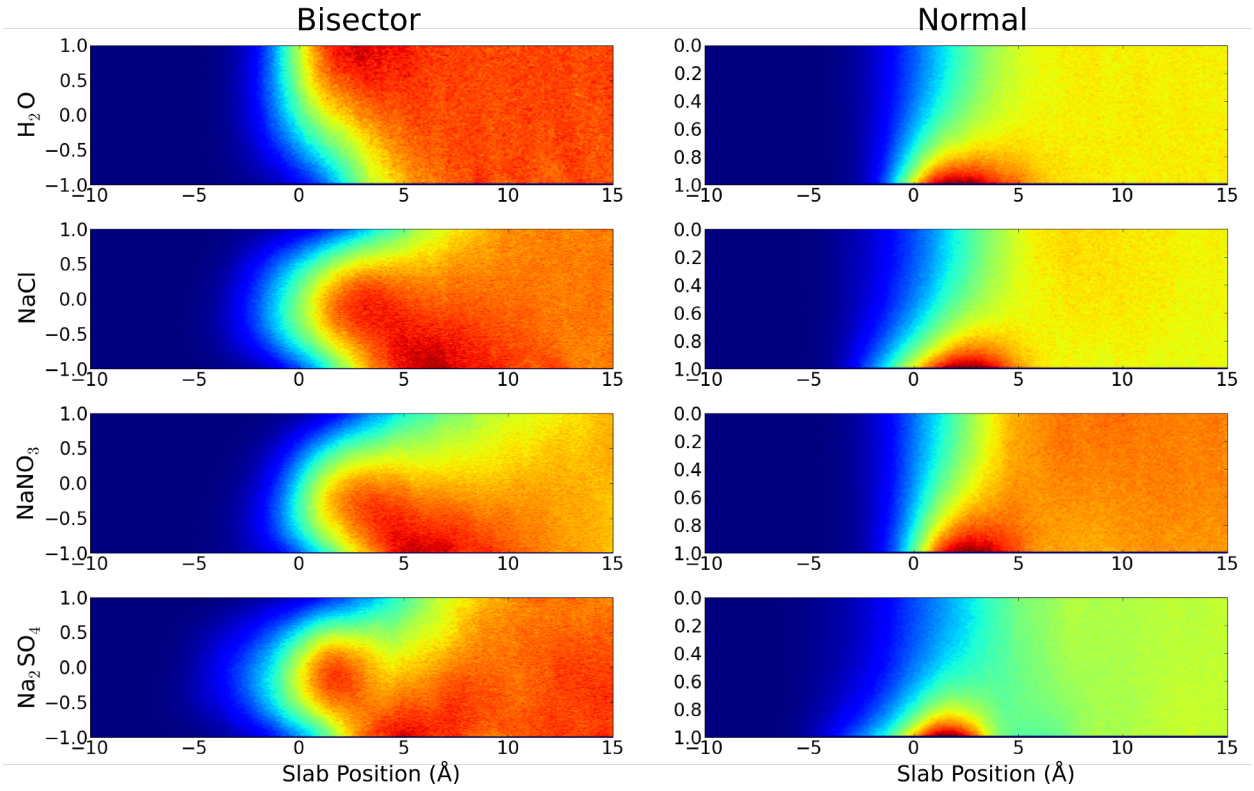

Figure. 3 — Orientation profiles of interfacial water molecules. Two profiles characterize the water orientation at different depths from the GDS (located at position 0.0). The molecular bisector profile (left) shows the orientation of the bisector with respect to the system reference axis (perpendicular to the plane of the interface). The profile of the molecular axis normal to the plane of the water molecule is also shown (right) with respect to the reference axis. Both angle definitions are depicted in figure 1, and the angle cosines are plotted here. The neat-H_2O , NaCl , $NaNO_3$, and Na_2SO_4 system water orientation profiles are plotted from top to bottom row, respectively.

Previous studies have provided a detailed overview of water orientation at the interface with both air and organic phases.[2,7,11,16,17] The topmost water layers are highly ordered because of their contact with the organic phase, and it has been suggested that ordering of both the organic and water molecules would lead to a field across the boundary of the interface.[2,7] This can influence charged species, and the ordering and orientation of the H-bond network. Our recent experimental SFG results suggest that the accumulation of charged ions leads to a field-screening that affects the orientation of waters in the topmost layers. This is complemented by the results of the current study.

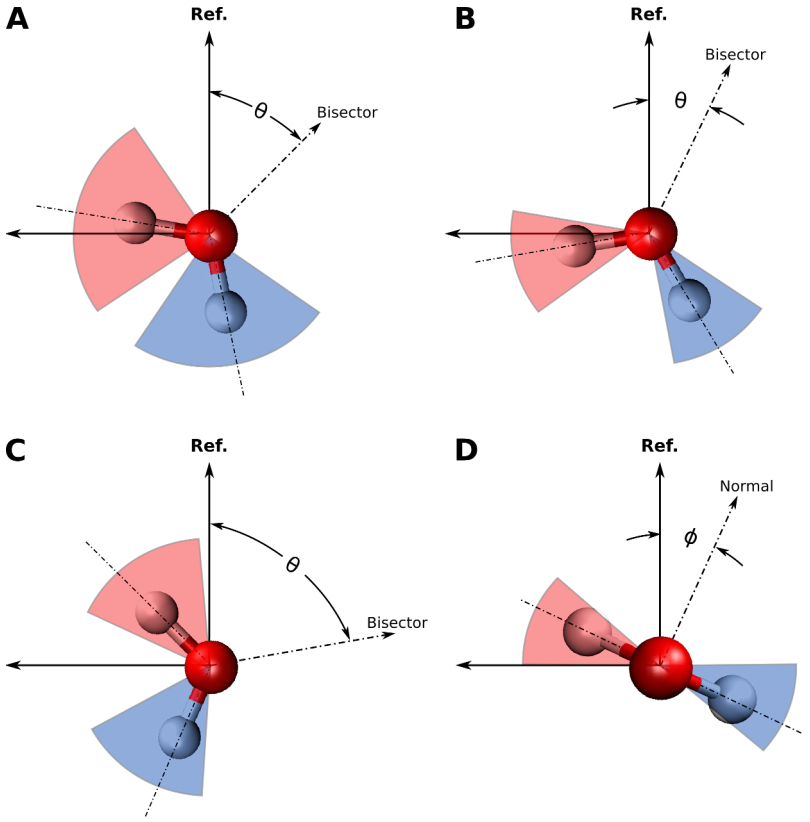

Figure. 4 — Depictions of various orientations for different ranges of the bisector and molecular plane normal angles (θ and ϕ, as shown in figure 1). The effect of rotating the water within a fixed angle range is illustrated by the shaded (red and blue) regions that bound the OH-bonds. Ranges of θ shown here are $0 < \cos\theta < 1$ (A), $0.7 < \cos\theta < 1$ (B), $-0.5 < \cos\theta < 0.5$ (C). The ϕ range of $0.7 < \cos\phi < 1$ (D) shows the molecular plane of the water mostly flat (i.e. parallel to) the plane perpendicular to the reference axis.

In the left column of figure 3 are the bisector orientation profiles for each of the systems. The far-left dark-blue regions of the plots show the CCl_4 bulk near to the interface where few or no waters are found. The GDS is located at a depth of 0.0 Å . To the far right in the water bulk, the flat, uniformly-colored profile

represents the expected isotropic orientation of the waters. The regions of interest lie around the GDS within the interface. The top bisector profile is that of the neat-H_2O system, and it shows a transition in the profile beginning just above the GDS and extending up to 5 Å into the aqueous side, at which point the profile becomes orientationally isotropic. At the GDS most of the waters are oriented between $0.0 < \cos\theta < 1.0$, indicating a range of orientation as depicted in figure 4a. In this range one of the OH-bonds points into the aqueous side, and the other straddles the interfacial plane with a slight affinity towards the organic CCl_4 phase. Just under the surface, between 2-4 Å into the neat-H_2O phase, a dark-red region spanning approx. $0.7 < \cos\theta < 1.0$ appears. This narrow orientational range is depicted in figure 4b, and is similar to the waters in the topmost aqueous layer nearer to the GDS, but limited such that both OH bonds point into the H_2O side, with one of them only straddling the interfacial plane with a tendancy to point into the H_2O phase.

The neat-H_2O bisector orientational profile is comparable to previous simulations of the same neat-H_2O reference system. Using different simulation parameters for the same neat-H_2O /CCl_4 system, Wick and Dang found the free-OH to point slightly into the CCl_4 phase at the GDS with an angle of $\cos\theta_{\ free-OH} \approx 0.4$. This corresponds to $\cos\theta_{\ bisector} \approx 0.5$ in the this work's angle definition. Similarly, deeper into the surface the angle profile dimishes such that $\cos(\theta_{free-OH}) \approx 0.0$ within 5 Å of the GDS, corresponding to $\cos(\theta_{bisector}) \approx 0.8$ in the current scheme. Those results agree with this work's neat-H_2O profile, further complementing the experimental SFG conclusions performed on the same systems.[7,40]

Bisector angle profiles for the salt systems show different behavior than that of the reference neat-H_2O system. The profiles of the salt systems at the GDS all center about the $\cos\theta = 0$ region, with a range of approx. $-0.5 < \cos\theta < 0.5$. This indicates a straddling water molecule with the orientational range depicted in figure 4c. The water in that range is clearly oriented such that one OH-bond always points out of the aqueous phase into the CCl_4 , and the other always points in to the water bulk. The OH-bond that would straddle the interface in the neat-water system points out of the interface with a greater angle. This orientation, centered about $\cos\theta \approx 0$, extends into the water phase up to 3 Å , at which point the profile shifts to the darker region near $-1.0 < \cos\theta < 0.7$. The sub-surface region of the profile between 4-7 Å in each system corresponds to a flip of the water orientation, as referred to in a recent SFG study as a "flip-flop" model where water orients to counteract the field of charged species at interfaces.[41] The cation density enhancement in each salt system is within the region of 5-7 Å below the GDS. The waters may be orienting with the negatively charged oxygen end towards those cations, and with the field established by the ion double-layer within the interface. In each of the salt bisector profiles there is a clear depletion of waters oriented towards $\cos\theta = 1$ suggesting that alignment of the bisector with the reference axis is not prefered. The effect is most pronounced in the Na_2SO_4 system where the distance between counterion density enhancements is smallest, and the transition in the bisector profile is the most abrupt, changing from a profile mostly in the range of $-1.0 < \cos\theta < 0.5$ to isotropic orientation quickly near 8 Å into the aqueous phase. The $NaNO_3$ system bisector profile shows the effect furthest into the water bulk, extending almost to 13 Å . Counterion density enhancement is most separated in $NaNO_3$, however, and most of the

orientational affinity for -1.0 $< \cos\theta <$ 0.5 occurs within the first 10 Å of the surface. The bisector profile of the NaCl system is broadest with -1.0 $< \cos\theta <$ 0.7 starting near the GDS. Also, orientational isotropy is shallowest in the NaCl system starting near 7 Å into the surface.

It appears that the field established by the anion-cation pairing within the interface affects the depth to which waters are oriented before the bulk isotropic profile begins. Also, the range of orientations beneath the surface is dependent on the properties of the anion. The weakly polarizable Cl^- anion does not restrict the orientational range as much as the more polarizable NO_3^- and SO_4^{2-} . Anions also appear to control the depth to which the water orientation is felt, with the most surface-active NO_3^- anion causing the deepest effect. SO_4^{2-} anion shows the strongest restriction on the range of bisector angles, and the sharpest orientational transition to the bulk, which may be attributed to the higher charge of the anion, and thus the stronger field established between the counterions in the system.

Orientational profiles for the molecular plane normal of the water molecules (ϕ-profiles) are found in the right-column of figure 3. The range of a ϕ-profileis limited to 0.0 $< \cos\phi <$ 1.0 because of the inherent symmetry of the plane of the water molecule. More similarity is shared between the ϕ-profiles than for the bisector profiles. The neat-H_2O profile is typical of the four profiles in appearance with a large clustering of water population in the range of 0.7 $< \cos\phi <$ 1.0 between the GDS and up to 7 Å into the aqueous phase. This particular ϕ range is depicted in figure 4d, showing the mostly flat (i.e. parallel to the interface) orientation of the molecular plane. It is noteable that the ϕ-orientation is affected to the same depth as the first peak (dark-red region) of the bisector profile. However, in the salt systems the second peak near to $\cos\theta = -1.0$ begin at a depth where the ϕ-profilehas already become isotropic. Thus, in the salt systems, the first water layer (between the GDS and almost 4 Å into the surface) has a defined ϕ-orientation that is rather flat on the interfacial plane, but the deeper waters (4-7 Å into the interface) are isotropic in ϕ, and oriented with $\cos\theta$ closer to -1.0 (an orientation with oxygen pointing into the water bulk, and hydrogens more towards the interface).

By virtue of the interdependence of θ and ϕ (the bisector is perpendicular to the molecular plane normal at all times) a value of $\cos\phi = 1.0$ implies $\cos\theta = 0$, and vice-versa. However, a broad θ-range allows for a full range of ϕ values. Although the second peak of the salt-system bisector profiles is concentrated near to $\cos\theta = -1.0$, the corresponding ϕ-profileis isotropic. This deeper region (the second water layer) orients with the bisector counteracting the field of the anion-cation double-layer, and the only apparent affinity is that of placing the oxygens closer to the cation density enhancement (and the hydrogens closer to the anion layer), while the ϕ-profilespans the entire orientational range.

5 Calculated Sum-Frequency Spectra

One of the aims of this simulation study is to complement our group's previous experimental SFG work.[7] The varied set of anions and their affect on the CCl_4 -H_2O interface is linked from theory to empirical data through the connection of computed SFG spectra. The computed spectra are presented in figure 5 along with the experimental spectra from our previous work with these same salt solutions.[7] On first look, the overall intensities and lineshapes follow remarkably similar trends as in the experimental systems. The key features of the CCl_4 -H_2O interfacial spectra are the diminished intensities below 3400 cm^{-1} as compared to previous liquid-air works, and the dominant "free-oh" peak near 3660 cm^{-1} .

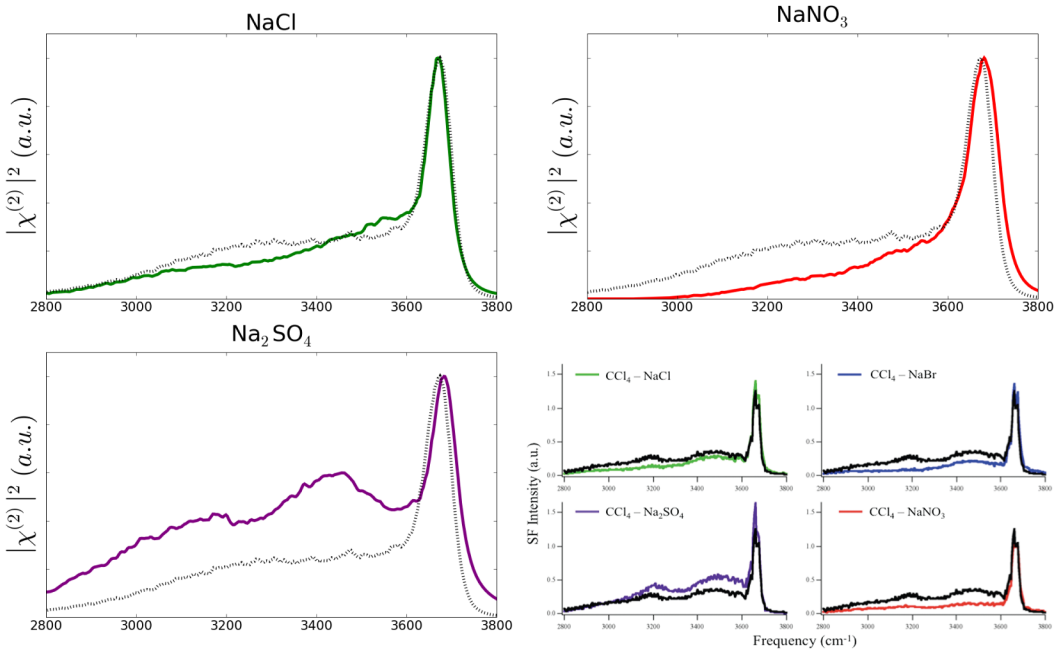

Figure. 5 — Vibrational SFG spectra of the water-OH stretching region for each interfacial aqueous-salt-CCl_4 system. The CCl_4 -H_2O interface spectrum (black-dashed line) is provided on each simulated SFG spectrum for reference. The bottom-right figure is a reproduction of the experimental spectra from McFearin et al to show the intensity and lineshape trends found experimentally for these systems.[7]

The reference CCl_4 -H_2O spectrum reproduces well the lineshape from experiment, but lacks the definition of the two peaks found near 3250 and 3450 cm^{-1} . These lower-frequency features have been attributed to the different H-bonding varieties of water that make up the more highly-coordinated, tetrahedral environments found deeper into the aqueous bulk. We have found difficulty in reproducing the lower-frequency peaks near

3200 cm^{-1} and attribute the slight differences in the lineshape to similar problems reported previously.[4] However, the lineshape is otherwise quite similar to that of the experiment, and warrants further comparison, suggesting that the methods are sound and justified for this study.

The presence of anions at the interface results in a "field-screening" that decreases the effect of the changing interfacial field further into the aqeous bulk. Water molecules found below the surface, those giving rise to the lower-frequency (i.e. below 3500 cm^{-1}) OH-stretch features, are thus less oriented by the field and their SFG contribution is decreased. Both the monovalent anions, Cl^- and NO_3^- , show this effect in their SFG spectra. Comparison to the reference neat-H_2O spectrum shows that the added presence of the surface-active anions decreases the lower-frequency intensities, as found in the experimental study. The Cl^- affects a notabely smaller decrease in the spectral intensities than the NO_3^- system. This expected result is most likely due to the higher preference for the surface of the larger, and more polarizable nitrate in the presence of CCl_4 . The NO_3^- ion is extremely surface active, as seen in the density profile, and should thus cause the greatest "field-screening" to waters found deeper in the bulk.

The divalent and larger SO_4^{2-} anion accumulates deeper into the aqueous bulk and exhibits the lowest surface affinity of the ions studied. This is likely due to the higher charge of the anion that leads to greater solvation. The sulfate provides little or no screening of the interfacial field from the top-most water layer, and only affects the deeper waters. Lower frequency features of the water OH-spectrum spectrum are noteably higher in intensity and both the 3250 and 3450 cm^{-1} features are present, and dominate as compared to the reference water system, in both the simulated and experimental spectra.

As concluded in the previous experimental work, the monovalent anions appear to screen the deeper water molecules from the field produced by the phase change at the aqueous-organic interface. Larger and more polarizable monovalent anions have a stronger screening effect due to their increased surface affinity. The large but more highly charged divalent anion experiences greater solvation and is thus found deeper in the aqueous phase. Deeper anions do not participate as field screening agents to the same extent as their monovalent counterparts, and the result is an increase across the lower frequencies of the water OH-stretching SFG spectrum.

6 Conclusions

We have simulated an interface between a neat-H_2O system and CCl_4 , as well as three aqueous salt systems with the same organic phase neighbors. By analyzing the density profiles of the water and the various ions in solution we found that anion behavior at the liquid-liquid boundary is different than at the air-liquid one. Anions that have been found to be depleted at the air-water interface such as NO_3^- have a strong interfacial affinity at the CCl_4 -H_2O interface. Similarly, the orientation of water molecules is different at the liquid-liquid interface when ions are present in solution. Depending on the ion surface affinity the waters orient to different extents and to different depths, supporting the conclusions of previous simulations and experiment. The field of interface simulation is further exposing the microscopic foundations of the macroscopic experimental results from techniques such as interface-specific spectroscopies. In our work we have connected the simulation results and methods by computing the SFG spectra to further complement previous experimental efforts. Further effort is still needed to provide a fuller understanding of the boundaries of aqueous systems and the effects of salt ions.

References

1. Hore, D. K.; Walker, D. S.; MacKinnon, L.; Richmond, G. L. *Journal of Physical Chemistry C* **2007,** *111,* 8832-8842.

2. Hore, D. K.; Walker, D. S.; Richmond, G. L. *Journal of the American Chemical Society* **2008,** *130,* 1800+.

3. Hore, D. K.; Walker, D. S.; Richmond, G. L. *Journal of the American Chemical Society* **2007,** *129,* 752-753.

4. Walker, D. S.; Hore, D. K.; Richmond, G. L. *Journal of Physical Chemistry B* **2006,** *110,* 20451-20459.

5. Walker, D. S.; Richmond, G. L. *Journal of the American Chemical Society* **2007,** *129,* 9446-9451.

6. Walker, D. S.; Moore, F. G.; Richmond, G. L. *Journal of Physical Chemistry C* **2007,** *111,* 6103-6112.

7. McFearin, C. L.; Richmond, G. L. *Journal of Physical Chemistry C* **2009,** *113,* 21162-21168.

8. Chang, T.; Peterson, K.; Dang, L. *Journal of Chemical Physics* **1995,** *103,* 7502-7513.

9. Eggimann, B. L.; Siepmann, J. I. *Journal of Physical Chemistry C* **2008,** *112,* 210-218.

10. Du, H.; Liu, J.; Ozdemir, O.; Nguyen, A. V.; Miller, J. D. *Journal of Colloid and Interface Science* **2008,** *318,* 271-277.

11. Wick, C.; Dang, L. *Journal of Physical Chemistry B* **2006,** *110,* 6824-6831.

12. Petersen, P.; Saykally, R.; Mucha, M.; Jungwirth, P. *Journal of Physical Chemistry B* **2005,** *109,* 10915-10921.

13. Matsumoto, M.; Kataoka, Y. *Journal of Chemical Physics* **1988,** *88,* 3233-3245 hyperbolic tangent fitting function for water density profiles.

14. Thomas, J. L.; Roeselova, M.; Dang, L. X.; Tobias, D. J. *Journal of Physical Chemistry A* **2007,** *111(16),* 3091-3098.

15. Wick, C. D.; Kuo, I.-F. W.; Mundy, C. J.; Dang, L. X. *Journal of Chemical Theory and Computation* **2007,** *3,* 2002-2010.

16. Fan, Y.; Chen, X.; Yang, L.; Cremer, P. S.; Gao, Y. Q. *Journal of Physical Chemistry B* **2009,** *113,* 11672-11679.

17. Wick, C. D.; Dang, L. X. *Chemical Physics Letters* **2008,** *458,* 1-5.

18. Galamba, N.; Cabral, B. J. C. *Journal of the American Chemical Society* **2008,** *130,* 17955-17960.

19. Ishiyama, T.; Morita, A. *Journal Of Physical Chemistry C* **2007,** *111,* 738–748.

20. Morita, A.; Hynes, J. *Chemical Physics* **2000,** *258,* 371-390.

21. Walker, D. S.; Richmond, G. L. *Journal of Physical Chemistry C* **2007,** *111,* 8321-8330.

22. Morita, A.; Hynes, J. *Journal of Physical Chemistry B* **2002,** *106,* 673-685.

23. Ishiyama, T.; Morita, A. *Journal of Physical Chemistry C* **2009,** *113,* 16299-16302.

24. Chang, T.; Dang, L. *Journal of Physical Chemistry B* **1997,** *101,* 10518-10526.

25. Dang, L. *Journal of Physical Chemistry B* **1999,** *103,* 8195-8200.

26. Hrobarik, T.; Vrbka, L.; Jungwirth, P. *Biophysical Chemistry* **2006,** *124,* 238-242.

27. Caldwell, J. W.; Kollman, P. A. *J. Phys. Chem.* **1995,** *99,* 6208-6219.

28. Rivera, J. L.; Starr, F. W.; Paricaud, P.; Cummings, P. T. *Journal of Chemical Physics* **2006,** *125,*.

29. Petersen, P.; Saykally, R. *Journal of the American Chemical Society* **2005,** *127,* 15446-15452.

30. Dang, L. *Journal of Physical Chemistry B* **1998,** *102,* 620-624.

31. Salvador, P.; Curtis, J. E.; Tobias, D. J.; Jungwirth, P. *Physical Chemistry Chemical Physics* **2003,** *5,* 3752–3757.

32. Chang, T.; Dang, L. *Journal of Chemical Physics* **1996,** *104,* 6772-6783.

33. Schnitzer, C.; Baldelli, S.; Shultz, M. *Journal of Physical Chemistry B* **2000,** *104,* 585-590.

34. Brown, M. A.; Winter, B.; Faubel, M.; Hemminger, J. C. *Journal of the American Chemical Society* **2009,** *131,* 8354.

35. Otten, D. E.; Petersen, P. B.; Saykally, R. J. *Chemical Physics Letters* **2007,** *449,* 261-265.

36. Xu, M.; Tang, C. Y.; Jubb, A. M.; Chen, X.; Allen, H. C. *Journal of Physical Chemistry C* **2009,** *113,* 2082-2087.

37. Wick, C.; Dang, L. X. *Journal of Chemical Physics* **2007,** *126,*.

38. Pegram, L. M.; Record, Jr., M. T. *Proceedings Of The National Academy Of Sciences Of The United States Of America* **2006,** *103,* 14278-14281.

39. Sloutskin, E.; Baumert, J.; Ocko, B. M.; Kuzmenko, I.; Checco, A.; Tamam, L.; Ofer, E.; Gog, T.; Gang, O.; Deutsch, M. *Journal of Chemical Physics* **2007,** *126,*.

40. Scatena, L.; Richmond, G. *Journal of Physical Chemistry B* **2001,** *105,* 11240-11250.

41. Nihonyanagi, S.; Yamaguchi, S.; Tahara, T. *Journal of Chemical Physics* **2009,** *130,*.